Supplementary information

Materials and methods

Materials

RPMI-1640 medium (HyCloneTM, Thermo Fisher Scientific), fetal bovine serum (Gibco, Thermo Fisher Scientific), Pen-Strep (HyCloneTM, Thermo Fisher Scientific) and β-mercaptoethanol (Sigma, USA) were used for cell culture. Phorbol 12-myristate 13-acetate (PMA; Sigma), lipopolysaccharide (LPS; Sigma), interferon-gamma (IFN-γ; ProSpec) and interleukin-4 (IL-4; PeproTech) were used for macrophage polarization. Pronase (Sigma, USA), collagenase IV (Sigma, USA), Hank's balanced salt solution (HyCloneTM, Thermo Fisher Scientific), deoxyribonuclease (Sigma, USA) and Percoll (GE Healthcare) were used for primary cell isolation. Human peripheral blood cell separation solution (TBDscience, China) was used for isolation of human peripheral blood-derived macrophages. Lipofectamine2000 Reagent (Invitrogen) was used for transfection. TRIzol™ reagent (Vazyme Biotech Co.,Ltd), Applied biosystems Veriti 96 wells thermal cycler (Thermofisher), Taq master mix (Vazyme Biotech Co.,Ltd), gDNA wiper mix and qRT super mix (Vazyme Biotech Co.,Ltd) were all used for RNA isolation and reverse transcription-polymerase chain reaction. RIPA lysis buffer (CWBio, China) and proteinase inhibitor cocktail (CWBio, China) were used for protein extraction. Exosome Concentration Kit (Rengen Biosciences Co.Ltd., China) was used for isolation of exosomes. CCl_4 (Sigma, USA) was used for mouse model.

Cell lines and cell culture

The human monocyte cell line THP-1 and human hepatic stellate cell line LX-2 were purchased from the Stem Cell Bank/Stem Cell Core Facility, SIBCB, CAS (Shanghai, China), and both cultured in RPMI-1640 medium containing 10% FBS, 1% Pen-Strep, while 0.05 mmol/L β-mercaptoethanol was added in THP-1 medium.

The cell-counting kit-8 assay (CCK-8)

LX-2 cells were seeded in 96-well plates ($3×10^3$ cells/well), and then treated with conditioned medium from different cells, such as M0 macrophages, M2 macrophages, or calcipotriol treated M2 macrophages. After cultured in conditioned medium, LX-2 cells were collected and detected the viability by CCK-8 assay. According to the manufacturer's protocol, the CCK-8 reagent was added to the cells in each well at 0 h, 12 h, 24 h, 36 h, 48 h after treatment, then incubated the cells at 37°C for 2 h. Measured the absorbance (optical density) at 450 nm to represent the viability of LX-2 cells.

RNA extraction and reverse transcription-polymerase chain reaction (RT-PCR)

Total RNA was extracted from cell culture media with TRIzol™ reagent according to manufacturer's instructions. The RNA was stored at −80 ℃ for subsequent assays. Reverse transcription and RT-PCR for RNA were performed using Applied biosystems Veriti 96 wells thermal cycler according the manufacturer's instructions. In brief, gDNA wiper mix and qRT super mix were added into RNA sample, followed by 50 ℃ reaction for 15 min. Then added Taq master mix and primers into system. After an initial denaturation step, the amplifications were carried out with 40 cycles.

Protein extraction and western blotting analysis

Total protein from cell or tissue was both extracted with RIPA lysis buffer

containing 1% proteinase inhibitor cocktail. Total protein was separated using 10% SDS-polyacrylamide gel electrophoresis and was electrophoretically transferred to polyvinylidene fluoride (PVDF) membranes. Then PVDF membranes were incubated with specific antibodies and fluorescein-conjugated secondary antibodies. Visualized immunoreactive bands by Tanon 5200 Multi and analyzed by ImageJ.

Small interfering RNA (siRNA) and plasmids transfection in vitro

The siRNA and plasmids were purchased from RIBOBIO Biotechnologies (Guangzhou, China). Transfection was carried out at a concentration of 50 nmol/L using Lipofectamine2000 Reagent. After transfection, the cells were cultured 24 h prior to terminal assays.

Nanoparticle Tracking Analysis (NTA)

The particle size and amounts of exosomes were measured by Malvern's NanoSight 300 (Malvern Instruments, U.K.). Specifically, particles were tracked using forward scattered 405 nm laser light, a 10× objective lens, and a CMOS camera. Temperature was held constant at 293 K for all experiments. A plastic syringe attached to a pump was used to flow diluted nanoparticle solutions through the imaging chamber between video collections to avoid any particle remained. Three videos of 30 s were collected for each sample. Then calculated the position of each particle in videos with NanoSight NTA 3.2 software.

Animal studies

All animals were treated in accordance with the Guide for Care and Use of Laboratory Animals, which was approved by the Animal Experimentation Ethics

Committee of China Pharmaceutical University. For CCl$_4$ induced hepatic fibrosis model, eight-week-old male C57BL/6J mice were IP injected CCl$_4$ once every two days for 4 weeks, with 0.5 ml/kg body weight (1:50 v/v in corn oil) or vehicle (DMSO in corn oil) as control. For bile duct ligation (BDL) induced hepatic fibrosis model, eight-week-old male C57BL/6J mice were anesthetized using isoflurane, and the common bile duct was ligated at the bifurcation near the liver hilum.

Calcipotriol was administered by oral gavage once every two days, with 20 μg/kg body weight, commencing 20 d after the first dose of CCl$_4$. The animals were terminated 72 h after the final CCl$_4$ injection.

Histology

Liver tissues were fixed in 4% paraformaldehyde buffered with neutral phosphate-solution. Then the fixed tissues were dehydrated in gradient ethanol, transparentized in xylene, and embedded in paraffin, sequentially. Embedded tissues were cut into sections at 5 μm thick, and were stained with hematoxylin-eosin (H&E; Solarbio) for structured observation, or with Masson's trichrome stain (Solarbio) for detection of collagen deposits.

Supplementary Tables

Table S1　Primer sequences for real-time PCR

| Primers	Forward (5' to 3')	Reverse (5' to 3')
IL-6	GAAACCGCTATGAAGTTCCTCTCTG	TGTTGGGAGTGGTATCCTCTGTGA
IL-1β	GAAATGCCACCTTTTGACAGTG	TGGATGCTCTCATCAGGACAG
TNF-α	CCTGTAGCCCACGTCGTAG	GGGAGTAGACAAGGTACAACCC
IL-10	AACTTGGCGCTCTACTTGCT	TAGCCGCCTGAGGACTTACT
MRC	CTCTGTTCAGCTATTGGACGC	TGGCACTCCCAAACATAATTTGA
CD163	ATGATGAGAGGCAGCAAGATGG	GCTACATGGCGGTGGAGACAA
Gapdh	TCAACAGCAACTCCCACTCTTCCA	TTGTCATTGAGAGCAATGCCAGCC
VDR	GCTGAACCTCCATGAGGAAG	GGATCATCTTGGCGTAGAGC
CYP24a1	GACCGCAAACAGCTTGATGTGGAT	ATATTCCTCACATCTTCCGCCCGT
COL1A1	ACTGCAACATGGAGACAGGTCAGA	ATCGGTCATGCTCTCTCCAAACCA
Timp	GGTGTGCACAGTGTTTCCCTGTTT	TCCGTCCACAAACAGTGAGTGTCA
U36B4	GCAGTGATGTAAAATTTCTTGG	AAA GCT CGGTTTTACTCTTCACA
β-actin	TGTCCACCTTCCAGCAGATGT	AGCTCAGTAACAGTCCGCCTAGA
SMAD2	ACCGAAGGCAGACGGTAACAAGTA	GACATGCTTGAGCAACGCACTGAA
SMAD3	ATGTCAACAGGAATGCAGCAGTGG	ATAGCGCTGGTTACAGTTGGGAGA

Supplementary Figures
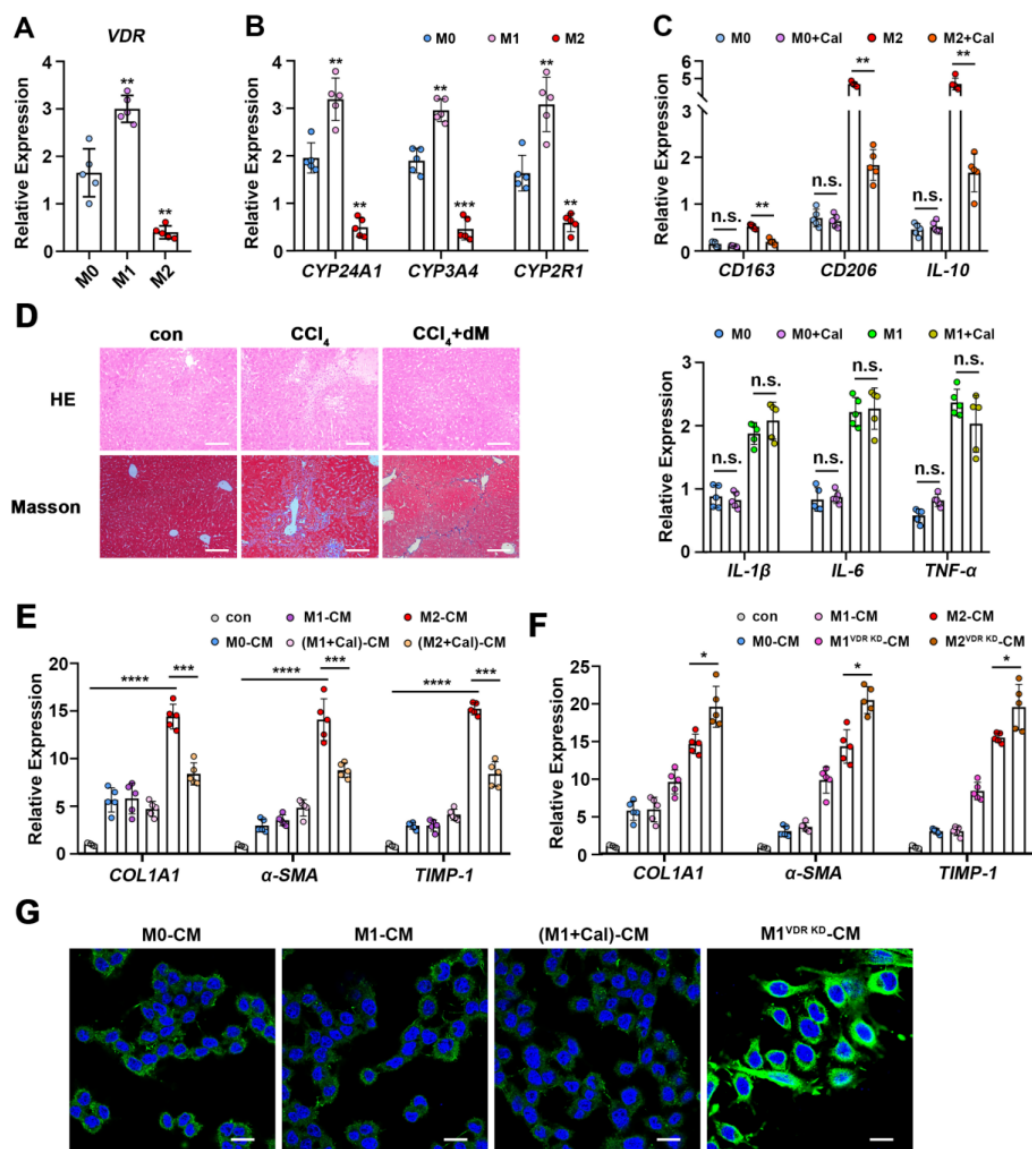
Fig. S1 VDR regulated the polarization of macrophages, leading to suppression of

HSC activation. (A) RT-PCR quantification of *VDR* in macrophages. *U36B4* was used

as the control. Data was mean±SEM (n=5). (B) RT-PCR quantification of *CYP24A1*,

CYP3A4 and *CYP2R1* in macrophages. *U36B4* was used as the control. Data was

mean±SEM (n=5). (C) RT-PCR quantification of *CD163*, *CD206*, *IL-10* in M2

macrophages (left) and *IL-1β*, *IL-6*, *TNF-α* in M1 macrophages. *U36B4* was used as the

control. Data was mean±SEM (n=5). (D) Effects of macrophage depletion on fibrosis

liver lesions and collagen deposition were determined by H&E staining and Masson's trichrome stain, respectively. Scale bar, 200 μm. (E) RT-PCR quantification of *COL1A1*, *α-SMA* and *TIMP* in LX-2. *U36B4* was used as the control. Data was mean±SEM (n=5). (F) RT-PCR quantification of *COL1A1*, *α-SMA* and *TIMP* in LX-2. *U36B4* was used as the control. Data was mean±SEM (n=5). (G) CLSM images of LX-2 cultured in different conditioned medium, co-stained for α-SMA (green) and Hoechst (blue), showed activation of LX-2. Scale bar, 5 μm. *P<0.05, **P<0.01, ***P<0.001.
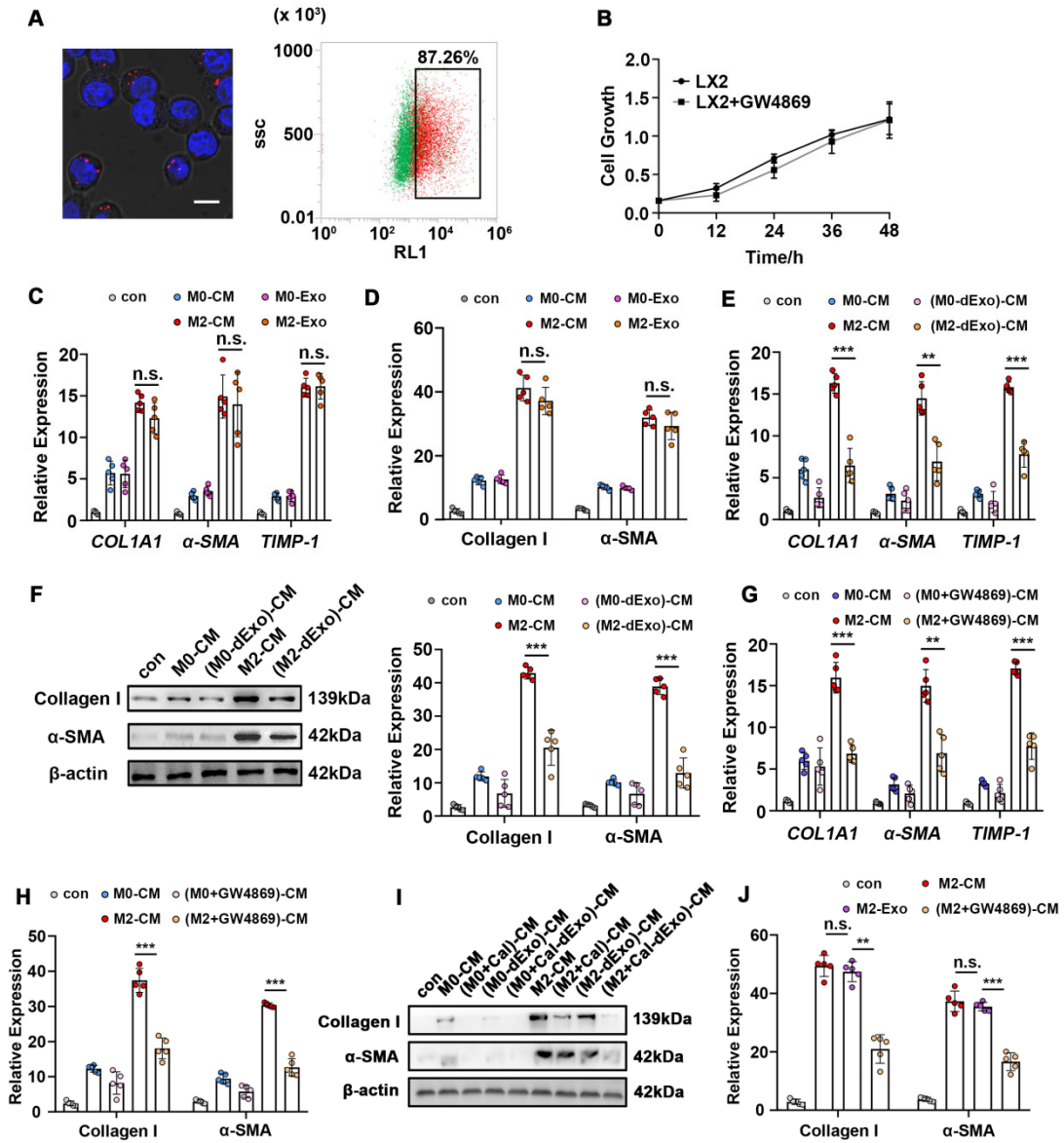
Fig. S2 Macrophage regulated activation of HSCs by exosomes. (A) CLSM images of LX-2 uptaking DiD-labeled exosomes. Nuclei were stained with hoechst (blue). Representative flow-cytometry dot plots of DiD staining for the exosomes-taken LX-2. LX-2 cells were treated with DiD-labeled exosomes for 24 h. Scale bar, 5 μm. (B) Cell growth curve of LX-2 treated with GW4869. Data was mean±SEM (n=6). (C) RT-PCR quantification of *COL1A1*, *α-SMA* and *TIMP* in LX-2. *U36B4* was used as the control. Data was mean±SEM (n=5). (D) Expression of collagen I and α-SMA in LX-2 treated

with different exosomes were examined by western blot, and protein expression levels were quantified by densitometry and normalized to the expression of β-actin. Data was mean±SEM (n=5). (E) RT-PCR quantification of *COL1A1*, *α-SMA* and *TIMP* in LX-2 treated with different conditioned medium. *U36B4* was used as the control. Data was mean±SEM (n=5). (F) Expression of collagen I and α-SMA in LX-2 treated with different conditioned medium were examined by western blot. Representative gel electrophoresis bands were shown, and protein expression levels were quantified by densitometry and normalized to the expression of β-actin. Data was mean±SEM (n=5) (G) RT-PCR quantification of *COL1A1*, *α-SMA* and *TIMP* in LX-2. *U36B4* was used as the control. Data was mean±SEM (n=5). (H) Expression of collagen I and α-SMA in LX-2 were examined by western blot, and protein expression levels were quantified by densitometry and normalized to the expression of β-actin. Data was mean±SEM (n=5). (I) Expression of collagen I and α-SMA in LX-2 treated with different conditioned medium were examined by western blot. Representative gel electrophoresis bands were shown. (J) Expression of collagen I and α-SMA in primary HSCs were examined by western blot, and protein expression levels were quantified by densitometry and normalized to the expression of β-actin. Data was mean±SEM (n=5). *P<0.05, **P<0.01, ***P<0.001.
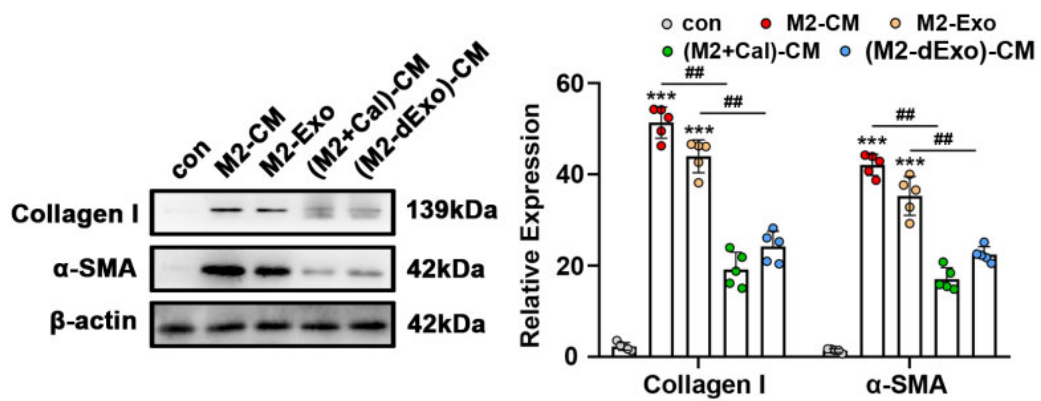
Fig. S3 Expression of collagen I and α-SMA in LX-2 treated with different medium were examined by western blot. Representative gel electrophoresis bands were shown, and protein expression levels were quantified by densitometry and normalized to the expression of β-actin. Data was mean±SEM (n=5). *P<0.05, **P<0.01, ***P<0.001, #P<0.05, ##P<0.01.
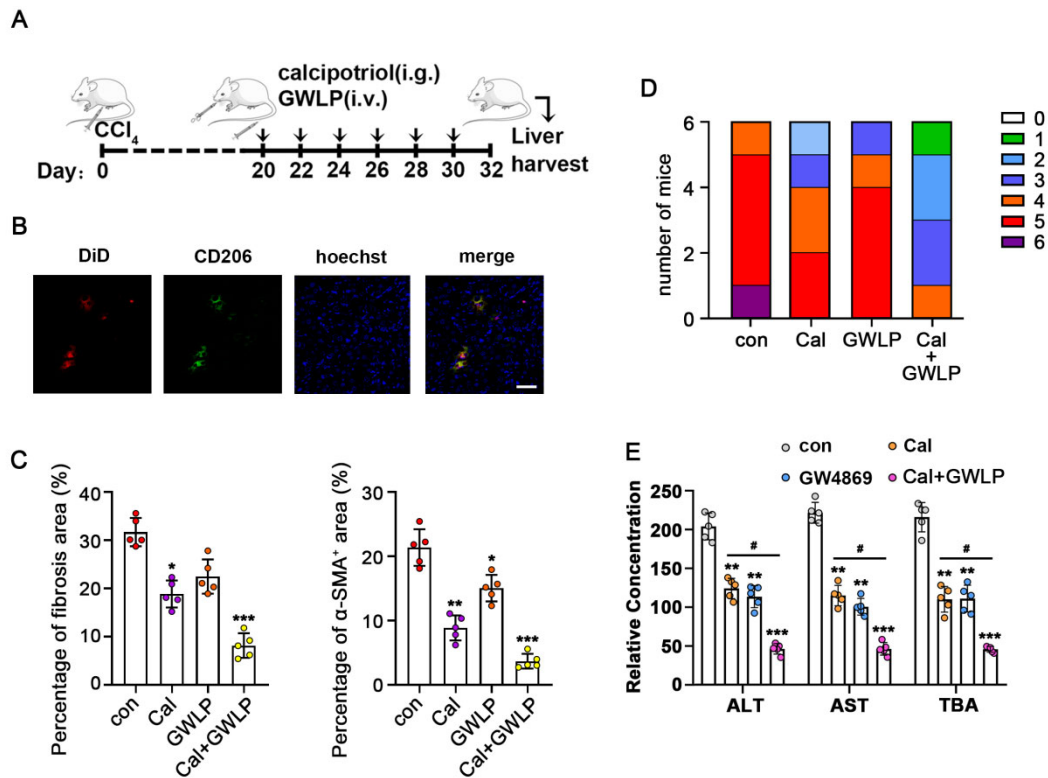
Fig. S4 Blockade of macrophage exosome secretion could inhibit CCl$_4$ induced hepatic fibrosis *in vivo*. (A) Treatment schedule for *in vivo* experiments. CCl$_4$ induced hepatic fibrosis mice was treated with GWLP by injection (i.v.) and calcipotriol administration by oral gavage once every two days, commencing 20 days after the first dose of CCl$_4$. Mice were sacrificed at day 32. (B) CLSM images of liver tissue sections from hepatic fibrosis model mice treated with DiD-labeled GWLP, co-stained for DiD (red), CD206 (green) and hoechst (blue), showed distribution of GWLP. Scale bar, 50 μm. (C) Quantification of fibrosis area in Masson's trichrome stain section and α-SMA positive area in immunofluorescence. Data was mean±SEM (n=5). (D) Ishak scoring criteria of different treated hepatic fibrosis model mice. Data was mean±SEM (n=6). (E) Serum levels of ALT, AST and TBA were determined. Data was mean±SEM (n=5). *$P<0.05$, **$P<0.01$, ***$P<0.001$. #$P<0.05$.
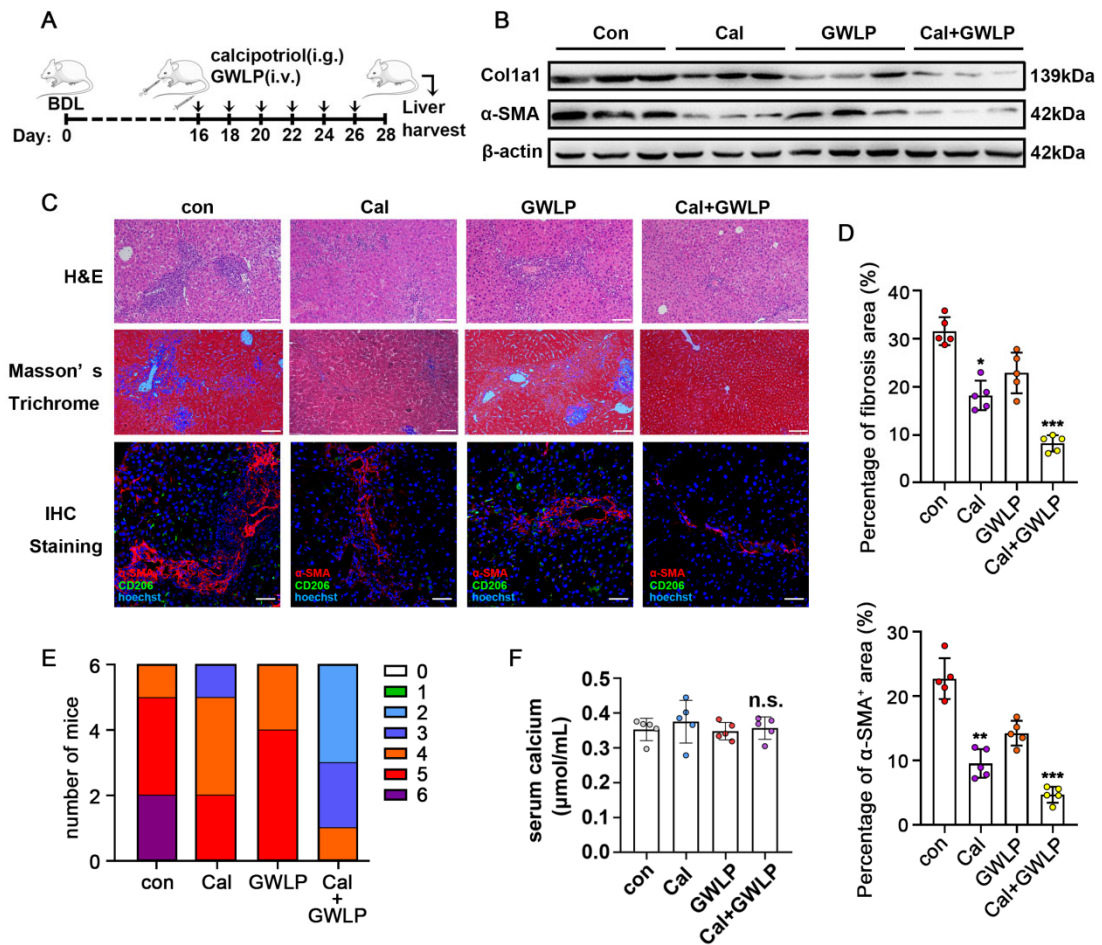
Fig. S5 Blockade of macrophage exosome secretion could inhibit BDL induced hepatic fibrosis *in vivo*. (A) Treatment schedule for *in vivo* experiments. BDL induced hepatic fibrosis mice was treated with GWLP by injection (i.v.) and calcipotriol administration by oral gavage once every two days, commencing 16 days after BDL. Mice were sacrificed at day 28. (B) Detection of protein expression with western blot analysis of collagen I and α-SMA in liver samples from different treated BDL model mice (left). β-actin was used as the control. Gray scale analysis was performed and quantification of collagen I/β-actin and α-SMA/β-actin were shown (right). Data was mean±SEM (n =5). (C) Effects of calcipotriol and GWLP inhibited the development of BDL-induced liver lesions, collagen deposition and a-SMA expression. Liver lesions

and collagen deposition were determined by H&E staining and Masson's trichrome stain, respectively. α-SMA expression was determined by immunofluorescence. H&E and Masson's trichrome stain: scale bar, 200 µm. CLSM images: co-stained for α-SMA (red) and hoechst (blue), scale bar, 50 µm. (D) Quantification of fibrosis area in Masson's trichrome stain section and α-SMA positive area in immunofluorescence. Data was mean±SEM (n=5). (E) Ishak scoring criteria of different treated hepatic fibrosis model mice. Data was mean±SEM (n=6). (F) Serum levels of calcium were determined. Data was mean±SEM (n=5). *$P<0.05$, **$P<0.01$, ***$P<0.001$.
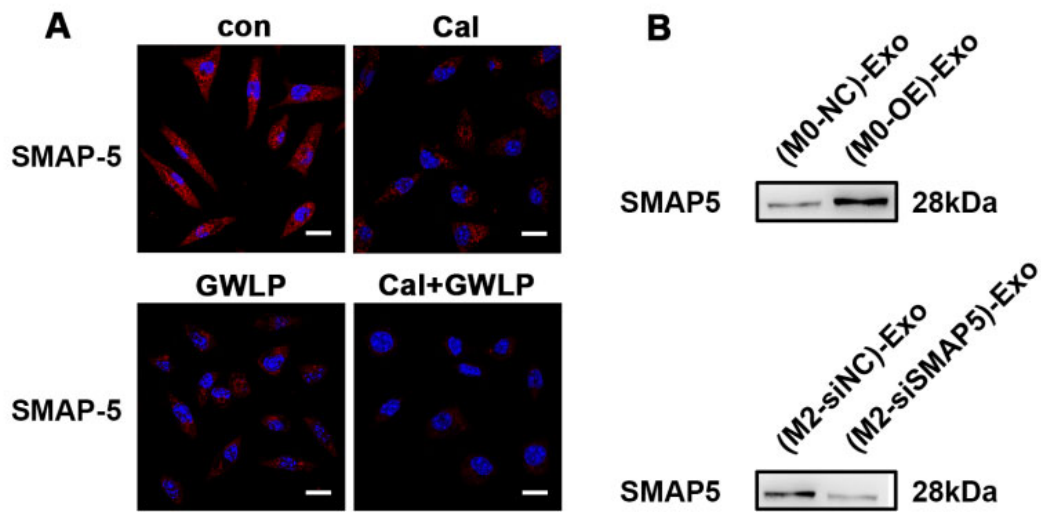
Fig. S6 Macrophage exosomal SMAP-5 could promote the activation of HSCs. (A) CLSM images of LX-2 treated with exosomes isolated from control M2 macrophages, calcipotriol and GW4869 treated M2 macrophages, co-stained for SMAP-5 (red) and hoechst (blue). Scale bar, 10 μm. (B) Expression of SMAP-5 in exosomes examined by western blot. Representative gel electrophoresis bands were shown.
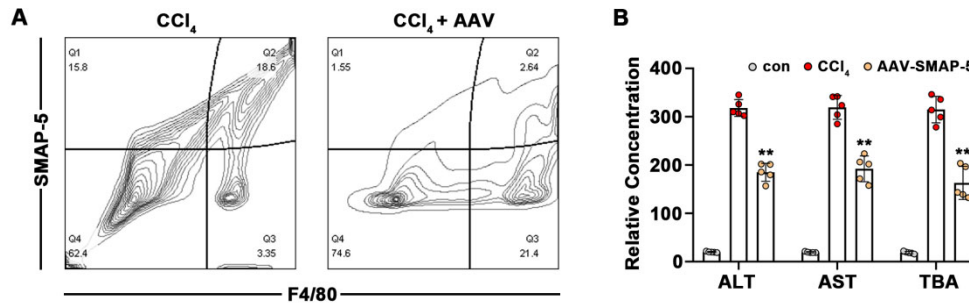
Fig. S7 (A) The validation of effectiveness of gene suppression via siRNA methodologies. Flow cytometry analysis of F4/80$^+$ SMAP-5$^+$ marophages and F4/80$^+$ SMAP-5$^-$ marophages after AAV-shSMAP-5 treatment, among all liver cells in CCl$_4$ induced hepatic fibrosis mice model, revealing the effectiveness of gene suppression via siRNA methodologies. (B) Serum levels of ALT, AST and TBA were determined. Data was mean±SEM (n=5). *$P<0.05$, **$P<0.01$, ***$P<0.001$.